

1 **Running Head:** Correlation of Microbial Communities with Travertine Mineral
2 Precipitation

3

4

5 **Correlation of Microbial Communities with Travertine Mineral Precipitation at**
6 **Mammoth Hot Springs, Yellowstone National Park, USA**

7 George T. Bonheyo¹, Jorge Frias-Lopez¹, Héctor García Martín², John Veysey², Nigel
8 Goldenfeld² and Bruce W. Fouke¹

9 *¹Department of Geology, University of Illinois at Urbana-Champaign, 1301 West Green*
10 *Street, Urbana, Illinois 61801-2938, USA.*

11 *²Department of Physics, University of Illinois at Urbana-Champaign, 1110 West Green*
12 *Street, Urbana, Illinois 61801-3080, USA.*

13

14

15 **Competing interests:** The authors have no competing interests that might be perceived
16 to influence the results and discussion reported in this paper.

17 **Correspondence** and request for materials should be addressed to Bruce W. Fouke
18 (Email: fouke@uiuc.edu).

1 **It is possible that common earth-surface geological features can arise as a result**
2 **of bacteria interacting with purely physical and chemical processes. The ability to**
3 **distinguish ancient and modern mineral deposits that are biologically influenced**
4 **from those that are purely abiotic in origin will advance our ability to interpret**
5 **microbial evolution from the ancient rock record on earth and potentially other**
6 **planets. We have combined carbonate mineralogical and geochemical environments**
7 **together with community-based microbial genetic analyses in hot spring drainage**
8 **systems at Mammoth Hot Springs in Yellowstone National Park. Previously (7), we**
9 **reported the shape and chemistry of carbonate mineral deposits (*travertine*), that**
10 **have formed along the hot spring pathways. This travertine exhibits five distinct**
11 **ecological zonations (termed sedimentary *facies*) even though most physical and**
12 **chemical attributes of the spring water change smoothly and continuously over the**
13 **course of the drainage outflow path. Here, we document an unexpectedly sharp**
14 **correlation between microbial phylogenetic diversity and travertine facies, which**
15 **suggests that changes in bacterial community composition are a sensitive indicator**
16 **of environmental conditions along the spring outflow. These results provide an**
17 **environmental context for constraining abiotic and biotic theories for the origin of**
18 **distinct crystalline structures and chemistries formed during hot spring travertine**
19 **precipitation.**

20

21

22

23

24

1 We have initiated a biocomplexity study at Mammoth Hot Springs in Yellowstone
2 National Park to determine whether microbial community structure and activity can
3 influence the chemistry and morphology of travertine mineral deposits (1, 2). Carbonates
4 are ideal for this type of study because they are precipitated at life-permitting
5 temperatures, are sensitive to environmental conditions, and are the most ubiquitous
6 sedimentary rocks at the Earth's surface (3 - 7). Subsurface waters erupt at Mammoth
7 Hot Springs to precipitate terraced crystalline travertine deposits composed of aragonite
8 and calcite (2, 7, 8, 9). Our studies were conducted at Spring AT-1 (7, 9), located on
9 Angel Terrace, in the upper terrace region of the Mammoth Hot Springs complex. Spring
10 AT-1 is typical of the hot springs found at Mammoth Hot Springs, in that as the spring
11 water flows away from the subsurface vent, the water cools, degases CO₂, increases in
12 pH, and precipitates travertine that steadily changes composition from nearly 100%
13 aragonite to nearly 100% calcite. Precipitation rates are rapid and can exceed 1.5 m per
14 year. The rapid precipitation partially seals the vents and reroutes surface flow paths,
15 causing the spring flow path to regularly change in direction and intensity, which in turn
16 influences subsequent travertine precipitation. The dynamical interplay between fluid
17 flow and precipitation (whether biotic or abiotic) is complex and not yet understood. The
18 hot springs harbor diverse communities of microorganisms, representing at least 21
19 divisions of bacteria (7).

20 In order to analyze the physical, geological, and biological aspects of this rapidly
21 changing hydrothermal system, it is necessary to first subdivide the spring drainage
22 system into a series of recognizable sub-environments along the flow path. These sub-
23 environments are known as sedimentary *facies*. A *facies* is defined by the sum of the
24 physical, chemical, geological, and biological attributes of an environment of
25 sedimentary deposition and mineral accumulation. Each *facies* has its own distinct
26 mineralogical and hydrological features and may therefore be readily identified, even if

1 the overall drainage system significantly changes and migrates. Our previous work
2 defined a five-component travertine depositional facies model for Spring AT-1 based on
3 physical characteristics (e.g. temperature and pH), appearance, mineralogy, and limited
4 microscopic observations of the microbiology (Fig. 1). These 5 facies are the vent, apron
5 and channel, pond, proximal slope, and distal slope (7, 9). The facies model allows
6 equivalent ecological locations in the spring drainage systems to be analyzed over time,
7 despite nearly constant changes in the rate or direction of spring flow, and thus allows
8 comparisons to be made between springs in different geographic locations and of
9 different geological ages.

10 Remarkably, we find that the physical structures characteristic of each facies develop
11 sharp boundaries instead of gradual transitional zones (7). Although any given travertine
12 facies may be as much as 10s of meters long and cover 100s of square meters in area, the
13 boundary between facies is relatively abrupt, occurring over as little as 1 cm in distance
14 between the pond (1-3 m in length along the spring flowpath) and proximal slope (10-15
15 m in length) or up to 10 cm between the proximal slope and distal slope (10-15 m in
16 length).

17 MATERIALS AND METHODS

18 **Field work and sample collection.** We collected multiple samples from within each
19 of the five travertine facies at Spring AT-1 for the purpose of conducting the first direct
20 correlation of bacterial 16S rRNA gene sequence identifications with travertine mineral
21 precipitation in the context of sedimentary depositional facies (7, 13). Field photographs
22 and detailed diagrams depicting aerial and cross-sectional views of Spring AT-1, and
23 sampling positions, have previously been published (7, 9). As a brief summary, samples
24 were collected from the interior of each of the five facies, with each sample occurring

1 within the continuous flow path of the primary hot spring drainage outflow. The sampling
2 strategy for the present study was to conduct an initial characterization of the microbial
3 communities inhabiting each travertine facies. Therefore, each sample was collected from
4 the middle of each facies and was thus laterally separated from the next sample by as
5 much as a few meters. With the results presented in this study and our previous work (7,
6 9), our ongoing microbiological analyses of Spring AT-1 is currently focused on detailed
7 mm-scale sampling across the boundaries between facies, as well as a correlation of
8 specific crystal morphologies and chemistries with microbial phylogenetic and functional
9 diversity. However, these next progressive and strategic stages of our analysis of Spring
10 AT-1 would not be possible without the synthesis of the data presented in the present
11 paper.

12 **DNA extraction, PCR amplification, cloning and sequencing.** The DNA
13 extraction protocols and 16S rRNA gene sequence PCR amplification protocols
14 employed have been optimized to avoid biases and have previously been described (7,
15 14). DNA amplified using universal bacterial primers was then cloned in order to isolate
16 the individual 16S rRNA gene sequences. To maximize the number of unique sequences
17 identified (thus better characterizing the total diversity of the spring system) we chose to
18 avoid sequencing identical clones derived from a single PCR reaction. Of the greater than
19 14,000 clones generated, approximately 5,000 clones were screened by RFLP analyses
20 and 1,050 potentially unique clones were selected for sequencing. Ultimately, 657 partial
21 16S rRNA gene sequences were obtained, and 108 of these were sequenced as contigs to
22 completion (15).

23 **Nucleotide sequence accession numbers.** The GenBank accession numbers for the
24 16S rRNA gene sequences analyzed in this study have previously been reported (7).

1 **Statistical analyses.** We analyzed our sequences using three Operational Taxonomic
2 Unit (OTU) definitions, defined by sequence differences of 0.5%, 1%, and 3%, to
3 determine whether our interpretations of environmental partitioning could be affected by
4 such variation. The lower bound is due to our PCR and sequence derived error rate (16,
5 17, 18) and the 3% difference is a typical OTU definition (19). In our accumulation
6 curves, a straight line would indicate that we have sampled only a small subset of the
7 total biodiversity: new OTUs are found at a constant rate with each additional new
8 sample analyzed. If a facies is well sampled, however, the curve will flatten
9 asymptotically when the number of samples, n , is large, because novel OTU sequences
10 are detected with decreasing frequency.

11 To quantitatively estimate how well each facies has been sampled, accumulation
12 curves were fitted to analytical curves obtained by modeling the sampling process. We
13 assume that in each environmental sample collected, there is a maximum of N possible
14 bacterial cells that could be detected, and that each of these cells would be present and
15 detected in the sample with a probability p , regardless of the cell's identity. The factor p
16 includes the combined probability of the cell being captured and detected through the
17 process of DNA extraction and amplification of the 16S rRNA gene sequences via PCR.
18 Thus, we use multiple methods of DNA extraction to eliminate cell durability biases and
19 amplify the 16S rRNA gene via PCR. Finally, we screen the resultant clone library in an
20 attempt to sequence only unique clones within that sample, as opposed to repeatedly
21 sequencing identical clones. In this manner we increase the likelihood that an OTU will
22 be detected even if it is not numerically dominant in the clone library (which may be due
23 to extraction, amplification, and cloning biases rather than environmental population
24 abundance).

1 The likelihood that each sequence we analyze will represent a new OTU is
2 approximated as $(1-S/S_o)$, where S is the number of different OTUs already identified and
3 S_o is the total number of different OTUs present in the environment. For each sequence,
4 the probability that the number of different OTUs will increase is $p(1-S/S_o)$. This leads to
5 an accumulation curve of the type $S=S_m (1-\exp(-Kt))$, where t is the maximum number of
6 individuals that would be found if $p=1$ and K is a constant related to the sampling
7 procedure. This is not quite what was represented in the accumulation curves, since we
8 only have information about samples rather than individuals, as explained above.
9 Nonetheless, the number of samples n is simply $n=t/N$, so $S=S_m (1-\exp(-Kn))$. The
10 parameters K and S_m were determined from a linear fit of $\log(dS/dn)$ versus $-n$. Estimates
11 through other methods were also attempted: fits to hyperbolic accumulation²⁴ curves
12 were not convincing and non-parametric methods^{25, 26} yielded variances that were too
13 large to be trustworthy.

14

15

RESULTS

16 We identified 193 OTUs using the 3% cutoff and found that 90% of these could be
17 identified in only one of the facies (partitioned between facies). There were 237 OTUs
18 using the 1% cutoff and 331 OTUs using the 0.5% cutoff with 91% and 93%
19 (respectively) of the sequences partitioning to a single facies. Figure 2 graphically
20 represents the distribution of sequences between the 5 facies using a 1% OTU definition.
21 The plots for the 3% and 0.5% definitions are similar in appearance; however, under the
22 3% rule, 2 sequences may be found in all 5 facies (20). Finally, the total number of
23 sequences that can be found in more than one facies remains low under each OTU
24 definition: 19 OTUs under the 3% definition, 20 OTUs under the 1% definition, and 24
25 OTUs under the 0.5% definition.

1 Accumulation curves were generated for the three different OTU definitions (3%,
2 1% and 0.5%) for each facies and the results for the pond facies are shown in Figure 3B.
3 The curve from each OTU definition collapses into the same curve, giving some
4 confidence in the robustness of the sampling procedure and the validity of the assumption
5 of random sampling used to derive the exponential accumulation curve. We see this
6 pattern no matter which OTU definition is used. In the model above, all of the OTUs
7 were assumed equally likely to appear (hence the factor $I-S/S_o$). In a more realistic model
8 the probability of finding each OTU should be proportional to its abundance. However,
9 the approximations used above describe the data well and provide a tractable expression
10 for the accumulation curve.

11

DISCUSSION

12 Although different microbial species have specific growth requirements and
13 preferred temperature and pH ranges, the tight partitioning with respect to the travertine
14 facies is nonetheless remarkable. First, it is surprising that very few of the upstream
15 sequences were not also detected downstream. We initially expected that the rapid flow
16 of the spring would result in downstream transport of microbial cells, and thus we
17 thought that many sequences would also be identified downstream of their point of
18 initial detection. Consequently, we performed most of our analyses on the first four facies
19 extending from the vent. Surprisingly, the sequences detected in the water column of one
20 facies, which are presumably most susceptible to being flushed downstream, were not
21 typically detected downstream of their original facies. Secondly, because bacterial
22 species have a preferred range of environmental growth conditions, we expected that
23 many sequences would be found across facies boundaries, coinciding with gradual
24 temperature and pH changes. However, the facies boundaries proved to be nearly
25 absolute boundaries with respect to detected bacterial 16S rRNA gene sequences.

1 Although we observed particular sequences over a range of conditions within each
2 travertine facies, with very few exceptions, OTUs were not found to traverse the facies
3 boundaries.

4 Inferred metabolic activity of the identified bacteria, derived from comparison of our
5 sequences to GenBank, indicates that the bacterial communities found in the spring
6 drainage system change from primarily chemolithotrophic in the vent facies, to
7 photoautotrophic and ultimately to heterotrophic in the distal slope facies. Associated
8 with this transition is an observed increase in the total number of OTUs and their
9 associated bacterial divisions from the vent to the pond facies. The number of OTUs
10 decreases, however, with down flow progression into the proximal slope and distal slope
11 facies. These trends in our data can be interpreted as follows: fewer OTUs and bacterial
12 divisions would be expected at the upper temperature limits of the spring where little
13 organic matter is available for heterotrophy and the temperature is at the upper limit for
14 photosynthesis (21). Although the pond through distal slope facies have temperature
15 profiles that would support both autotrophic and heterotrophic lifestyles, we actually find
16 a reduction in the number of species represented in the proximal slope and distal slope.
17 Although unproven, we hypothesize that such variation may result from differences in the
18 environmental stability of each facies with regards to temperature, pH, and water flow.
19 Ponds, for example, have the widest temperature and pH range of any facies and show
20 greater fluctuations in flow direction and intensity.

21 To validate our interpretation of facies partitioning, we need to determine what
22 proportion of the total community in each facies we have identified. Severe under-
23 sampling might prevent us from identifying OTUs that actually do occur in multiple
24 facies. Estimates for the total number of OTUs in each facies are made using an
25 exponential fit to the accumulation curve in Figure 3 (22). The accumulation curve plots

1 the number of different OTUs, S , found in a given number of samples versus this number
2 of samples, n . Since all of the samples are assumed to be equivalent, this graph is an
3 average over all possible permutations of these samples. Accumulation curves are
4 traditionally made using the number of individuals as the x-axis instead of the number of
5 samples²³. However, our samples amalgamate large numbers of individuals: we have
6 information regarding which OTUs are present in each sample, but not the OTU identity
7 for every individual in the sample. The abundance of unique gene sequences in the clone
8 libraries are not representative of the abundances in the environmental sample due to the
9 inherent DNA extraction and PCR biases. Therefore, the clone library data cannot be
10 used to make accumulation curves.

11 Accumulation curves were generated based on the three different OTU definitions
12 (3%, 1% and 0.5%) for each facies, with the results for the pond facies shown as an
13 example in Figure 3B. The curve from each OTU definition collapses into the same
14 curve, giving confidence in the robustness of the sampling procedure and the validity of
15 the assumption of random sampling used to derive the exponential accumulation curve.
16 Thus, since all of the individual cells are captured with equal probability, we expect that
17 the observed OTUs represent the most numerically abundant bacteria in each facies.
18 Consequently, we conclude that these species (and therefore most of the bacterial
19 consortia) are partitioned according to the travertine facies model. This finding constrains
20 abiotic theories for the origin of travertine terraces: either the origin is biotic, or else the
21 microbial ecology is strongly coupled to the geochemistry through mechanisms presently
22 unknown.

23

ACKNOWLEDGEMENTS

24 This research was supported by grants from the NSF Biocomplexity in the Environment
25 Program, NSF Geosciences Postdoctoral Research Fellowship Program, Petroleum

1 Research Fund of the American Chemical Society Starter Grant Program, and the
2 University of Illinois Urbana-Champaign Critical Research Initiative. Discussions with
3 A. Salyers and C. Woese are gratefully acknowledged.

4

5

REFERENCES

6

1. Northrup, D, Lavoie, K.H. 2001. Geomicrobiology of caves: a review.

7

Geomicrobiology J. **18**, 199-221.

8

2. Ford, T.D., Pedley, H.M. 1996. A review of tufa and travertine deposits of the world.

9

Earth Sci. Rev. **41**, 117-175.

10

3. Friedman, I. 1970. Some investigations of the deposition of travertine from hot

11

springs: I. The isotope chemistry of a travertine-depositing spring. *Geochim.*

12

Cosmochim. Acta, **34**, 1303-1315.

13

4. Given, R.K. & Wilkinson, B.H. 1985. Kinetic control of morphology, composition,

14

and mineralogy of abiotic sedimentary carbonates. *J. Sed. Petrology*, **55**, 109-119.

15

5. Chafetz, H.S., Ruxh, P.F., Utech, N.M. 1991. Microenvironmental controls on

16

mineralogy and habit of CaCO₃ precipitates: an example from an active travertine

17

system. *Sedimentology*, **38**, 107-126.

18

6. Burton, E.A. 1993. Controls on marine carbonate cement mineralogy: review and

19

reassessment. *Chem. Geol.*, **105**, 163-179.

20

7. Fouke, B.W., Bonheyo, G.T., Sanzenbacher, B.L., Frias-Lopez, J. 2003. Partitioning

21

of bacterial communities between travertine depositional facies at Mammoth Hot

22

Springs, Yellowstone National Park, U.S.A. *Can. J. Earth Sci.*, **40**, 1531-1548 p.

- 1 8. Sorey, M.L. 1991. Effects of potential geothermal development in the Corwin Springs
2 known geothermal resources area, Montana, on the thermal features of Yellowstone
3 National Park. 91-4052 (U.S. Geological Survey, Menlo Park, CA).
- 4 9. Fouke, B.W. Farmer, J.D., Des Marais, D.J., Pratt, L., Sturchio, N.C., Burns, P.C.,
5 Discipulo, M.K. 2000. Depositional facies and aqueous-solid geochemistry of
6 travertine-depositing hot springs (Angel Terrace, Mammoth Hot Springs,
7 Yellowstone National Park, USA). *J. Sed. Res.*, **70**, 265-285.
- 8 10. Farmer, J.D. 2000. Hydrothermal systems: doorways to early biosphere evolution.
9 *GSA Today*, **10**, 1-8.
- 10 11. Benson, L., White, L.D., Rye, R. 1996. Carbonate deposition, Pyramid Lake
11 subbasin, Nevada: 4. Comparison of stable isotope values of carbonate deposits
12 (tufas) and the Lahontan lake-level record. *Palaeogeography, Palaeoclimatology,*
13 *and Palaeoecology*, **122**, 45-76.
- 14 12. Boston, P.J. 2001. Cave biosignature suites: microbes, minerals and Mars.
15 *Astrobiology*, **1**, 25-55.
- 16 13. The sampling regime included filtering 2 liters of water collected from each facies,
17 sampling microbial masses, and sampling from the uppermost 1 cm of travertine
18 deposits.
- 19 14. Frias-Lopez, J., Zerkle, A.L., Bonheyo, G.T., Fouke, B.W. 2002. Cyanobacteria
20 diversity associated with coral black band disease in Caribbean and Indo-Pacific
21 reefs. *Appl. Environ. Microbiol.*, **69**, 2409-2413.
- 22 15. A complete file of all of the sequences identified and their GenBank accession
23 numbers is available as Tables 1 and 2 in the supplementary material, to be made
24 available online.

- 1 16. Sequence and PCR error rate: Repetitive single-stranded sequencing and editing of
2 the same sequences gave a predicted error rate of 0.32% and the error rate for Taq
3 polymerase is 10^{-4} (17, 18).
- 4 17. Tindall, K.R., Kunkel, T.A. 1988. Fidelity of DNA synthesis by the *Thermus*
5 *aquaticus* DNA polymerase: *Biochemistry*, **27**, 6008-6013.
- 6 18. Barnes, W.M. 1992. The fidelity of Taq polymerase catalyzing PCR is improved by
7 an N-terminal deletion. *Gene*, **112**, 29-35.
- 8 19. Stackebrandt, E., Goebel, B. 1994. Taxonomic Note: a place for DNA-DNA
9 reassociation and 16S rRNA sequence analysis in the present species definition in
10 bacteriology. *Int. J. Syst. Bacteriol.* **44**, 846-849.
- 11 20. Plots for 3% and 0.5% OTU definitions are included as Figure 1 in the
12 supplementary material, to be made available online.
- 13 21. Miller, S.R., Castenholz, R.W. 2000. Evolution of thermotolerance in hot spring
14 cyanobacteria of the genus *Synechococcus*. *Appl. Environ. Microbiol.* **66**, 4222-
15 4229.
- 16 22. Additional plots for the other facies and OTU definitions are found in Figures 2-4 of
17 the supplementary material, to be made available online.
- 18 23. Hughes, J.B., Hellmann, J.J., Ricketts, T.H., Bohannan, B.J.M. 2001. Counting the
19 uncountable: statistical approaches to estimating microbial diversity. *Applied and*
20 *Environmental Microbiology* **67**, 4399-4406.
- 21 24. Colwell, R. K., Coddington, J.A. 1994. Estimating terrestrial biodiversity through
22 extrapolation. *Philosophical Transactions of the Royal Society (Series B)* **345**, 101.
- 23 25. Krebs, C. 1989. *Ecological methodology* (Harper and Row, New York).

- 1 26. Chao, A. and Lee, S-M. 1994. Estimating population size via sample coverage for
- 2 closed capture-recapture models, *Biometrics* **50**, 88.

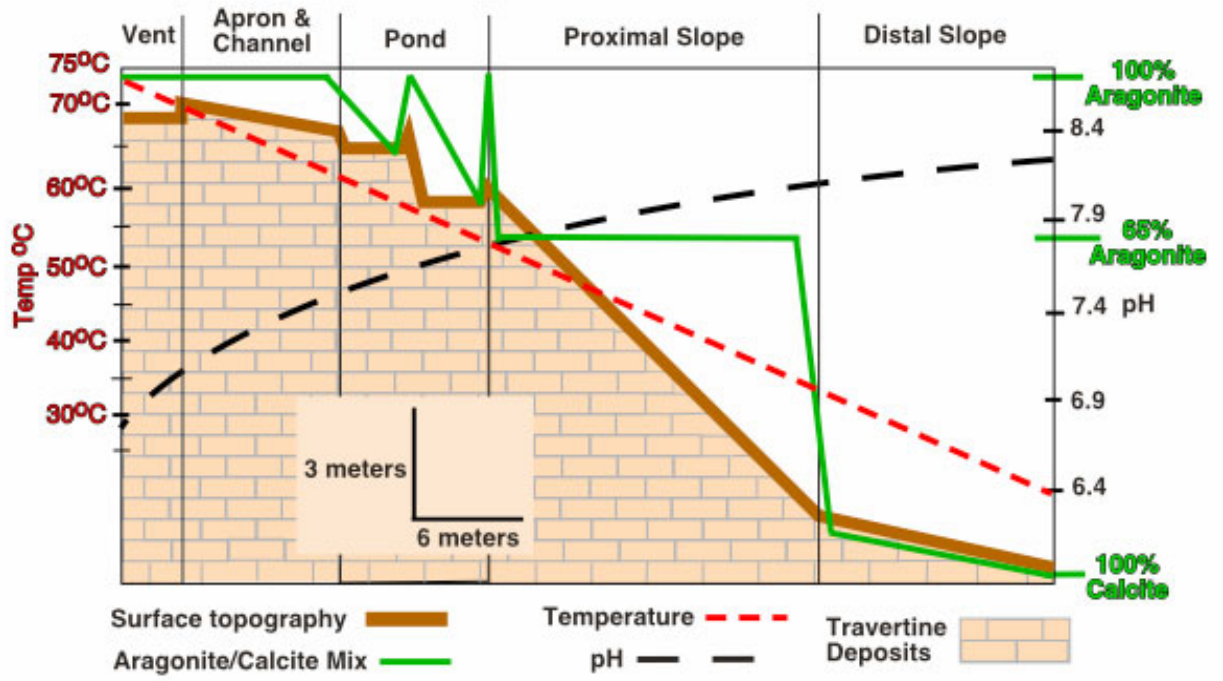
1 **Fig 1.** Facies model. Cross-sectional view of Spring AT-1 with 2x vertical exaggeration
2 to highlight the topography of the spring features. Trends in pH, temperature and
3 travertine aragonite/calcite mineralogical ratios overlay the structural representation to
4 show how these attributes change with increasing distance from the spring outflow source
5 vent.

6

7 **Fig. 2.** Species present in each facies: 1% OTU definition. Each OTU is numbered
8 sequentially, starting with OTUs that first appear in the Vent facies, followed by OTUs
9 that first appear in the Apron and Channel, then the Pond, the Proximal Slope, and lastly
10 the Distal Slope facies. The figure provides a graphical representation of where each
11 OTU (*y*-axis) is found (*x*-axis).

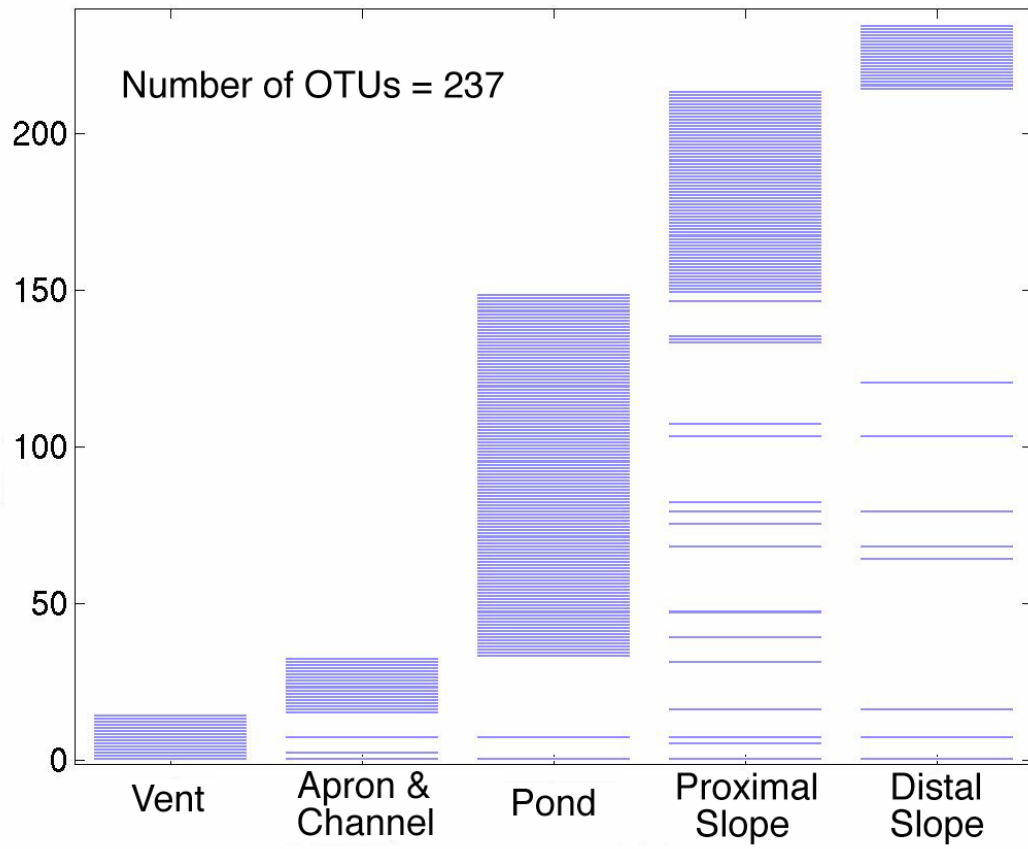
12

13 **Fig. 3.** Accumulation curves and exponential fits. **(A)** Accumulation curve generated for
14 each facies using a 1% OTU definition. **(B)** Accumulation curves generated for the pond
15 facies using a 3%, 1%, and 0.5% OTU definitions. Accumulation curves for different
16 OTU definitions collapse into the same curve when the *x* and *y*-axis are properly scaled
17 by the total number of OTUs and samples, respectively.



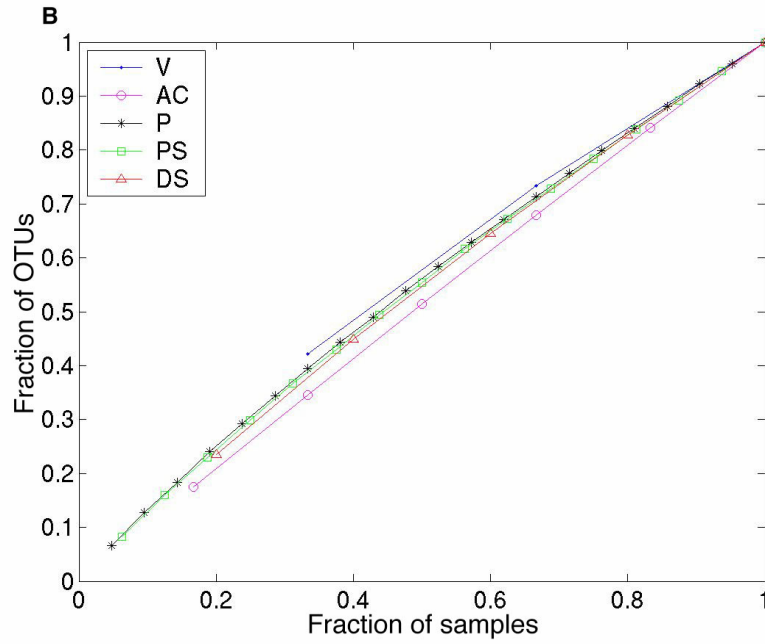
1

2 Figure 1



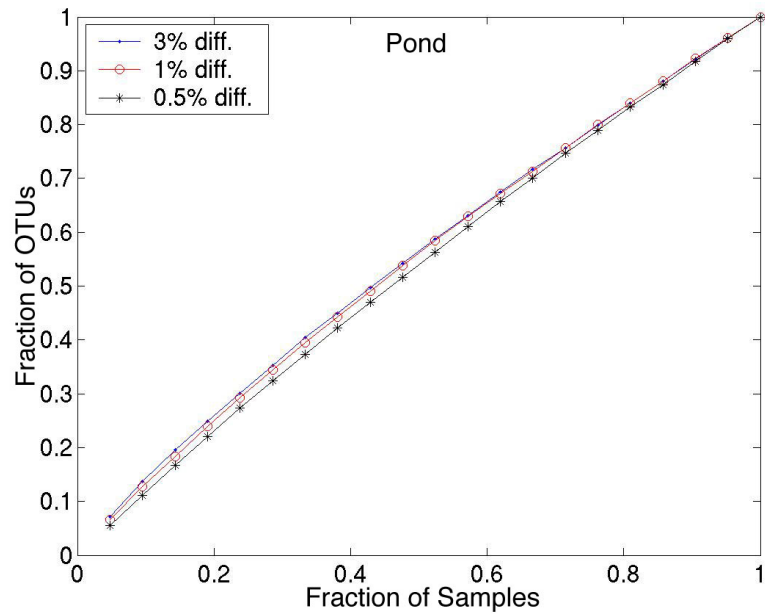
1

2 Figure 2.



1 Fig 3A

2



3 Fig 3B

4